Supplementary Material

Fabrication of Flexible Quasi-Interdigitated Back-Contact Perovskite Solar Cells

Hryhorii P. Parkhomenko [1], Erik O. Shalenov [1,2], Zarina Umatova [1], Karlygash N. Dzhumagulova [1,2] and Askhat N. Jumabekov [1,*]

[1] Department of Physics, Nazarbayev University, Nur-Sultan 010000, Kazakhstan; hryhorii.parkhomenko@nu.edu.kz (H.P.P.); shalenov.erik@mail.ru (E.O.S.); umatovazarina2101@gmail.com (Z.U.); dzhumagulova.karlygash@gmail.com (K.N.D.)
[2] Institute of Experimental and Theoretical Physics, Al-Farabi Kazakh National University, Almaty 050040, Kazakhstan
* Correspondence: askhat.jumabekov@nu.edu.kz

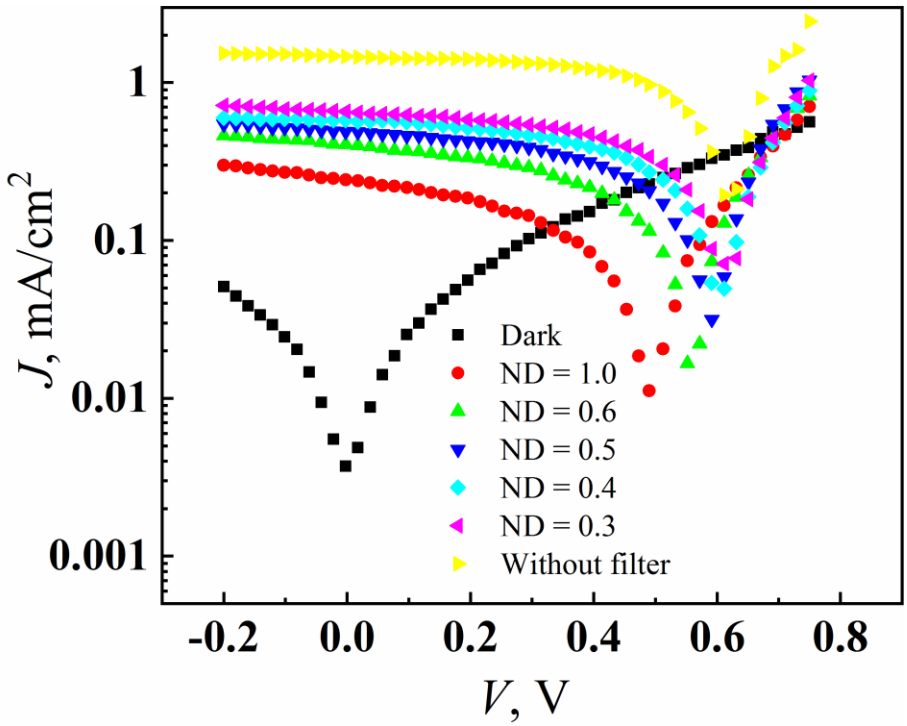

Figure S1. *J-V* curves of a FQIBC PSC for the front-side illumination and different light intensities.

Experimental Details

Standard drift-diffusion model, employing the Shockley-Read-Hall (SRH) recombination rate is used to simulate behavior and performance of back-contact perovskite solar cells (BC-PSCs)

with flexible quasi-interdigitated electrodes. To calculate the *J-V* curves of devices, the following system of equations [1] was solved for given device architecture, geometry, and physical parameters of the device functional layers:

1. Poisson Equation:

$$\nabla \cdot \left(-\varepsilon_0 \varepsilon_r \nabla V\right) = \rho(x,y,z), \qquad \text{(Equation S1)}$$

where $\rho(x,y,z) = q\left(p(x,y,z) - n(x,y,z) + N_d^+(x,y,z) - N_a^-(x,y,z)\right)$ with corresponding boundary conditions specific to the device architecture, $p(x,y,z), n(x,y,z), N_d^+(x,y,z), N_a^-(x,y,z)$ are local concentrations of charge carriers, acceptors, and donors, respectively.

Values of the equilibrium concentration of charge carriers are obtained from the following equations:

$$\begin{aligned} n &= \frac{1}{2}\left(N_d^+ - N_a^-\right) + \frac{1}{2}\sqrt{\left(N_d^+ - N_a^-\right)^2 + 4n_i^2} \\ p &= -\frac{1}{2}\left(N_d^+ - N_a^-\right) + \frac{1}{2}\sqrt{\left(N_d^+ - N_a^-\right)^2 + 4n_i^2} \end{aligned}, \qquad \text{(Equation S2)}$$

Here,

$$n_i = \sqrt{N_{c0} N_{v0}}\exp\left(-\frac{E_g}{2k_B T}\right), \qquad \text{(Equation S3)}$$

is the intrinsic concentration of charge carriers and N_{c0}, N_{v0} are the effective density of states in the conduction and valence bands. For the determination of local concentrations at given device geometry, the profiles of the concentrations at the junctions needs to be chosen accurately.

2. Charge carrier currents for electrons and holes:

$$\begin{aligned} &\nabla \cdot J_n = 0, \nabla \cdot J_p = 0 \\ &J_n = qn\mu_n E_c + \mu_n k_B T \nabla n \ , \\ &J_p = qn\mu_p E_v + \mu_p k_B T \nabla p \end{aligned} \qquad \text{(Equation S4)}$$

where, $E_c = -\nabla\left(V + \chi_0\right), E_v = -\nabla\left(V + \chi_0 + E_{g,0}\right)$, $E_{g,0}$ is band gap, χ_0 - electron affinity, μ_n - mobility of electrons, and μ_p mobility of holes.

3. Continuity equations:

$$\begin{aligned} &\frac{\partial n}{\partial t} = G_n - R_n + \frac{1}{q}\nabla \cdot J_n \\ &\frac{\partial p}{\partial t} = G_p - R_p - \frac{1}{q}\nabla \cdot J_p \end{aligned} \ , \qquad \text{(Equation S5)}$$

here, G_n, G_p - unit volume generation rate for electrons and holes, R_n, R_p recombination rates (Shockley-Read-Hall). The Shockley-Read-Hall recombination rate [2,3] is detrained as following:

$$\begin{aligned} &R_n = \frac{np - n_i^2}{\tau_p\left(n + n_1\right) + \tau_n\left(p + p_1\right)} = R_p, \\ &\nabla \cdot J_n += qR_n, \nabla \cdot J_p += R_p \end{aligned} \qquad \text{(Equation S6)}$$

where τ_p and τ_n are lifetimes for holes and electrons.

Spatial and wavelength dependent carrier generation rate is obtained by the following relationship:

$$g(x,y,z,\lambda) = \alpha(x,y,z,\lambda)\varphi(\lambda)P_s(x,y,z,\lambda) \qquad \text{(Equation S7)}$$

Here, $\alpha(x,y,z,\lambda)$ is the absorption coefficient and $\varphi(\lambda)$ is the solar incident photon flux (AM1.5G), and $P_s(x,y,z,\lambda)$ is the power flow. $P_s(x,y,z,\lambda)$ is calculated by the following relations:

$$P_s(x,y,z,\lambda) = \sqrt{|P_{ox}(x,y,z,\lambda)|^2 + \left|P_{oy}(x,y,z,\lambda)\right|^2 + |P_{oz}(x,y,z,\lambda)|^2} \qquad \text{(Equation S8)}$$

where,

$$P_{ox}(x,y,z,\lambda) = \tfrac{1}{2}Re\left(E_y H_z^* - E_z H_y^*\right) \qquad \text{(Equation S9a)}$$

$$P_{oy}(x,y,z,\lambda) = \tfrac{1}{2}Re(E_z H_x^* - E_x H_z^*) \qquad \text{(Equation S9b)}$$

$$P_{oz}(x,y,z,\lambda) = \frac{1}{2}Re\left(E_x H_y^* - E_y H_x^*\right) \quad \text{(Equation S9c)}$$

Here, E and H represent the spatially and frequency dependent electric and magnetic fields yielded by incident light. The symbols "Re" and "$*$" are the operators for taking the real part and the complex conjugation, respectively. The carrier generation rate is calculated by the following relationship:

$$G(x,y,z) = \int_{\lambda_1}^{\lambda_2} g(x,y,z,\lambda)d\lambda \quad \text{(Equation S10)}$$

Here, λ_1 is set to 300 nm and λ_2 is set to 800 nm.

Table S1. Physical parameters used for simulation experiments [4–11].

Parameters and units	**ZnO (ETL)**		**$MAPbI_3$ (Perovskite)**	
	Ideal	**Adjusted**	**Ideal**	**Adjusted**
Dielectric constant	9	9	30	6.5
Band gap (eV)	3.4	3.4	1.55	1.55
Electron affinity (eV)	4.4	4	3.9	3.9
Electron mobility ($cm^2/V{\cdot}s$)	10	10	50	1.4
Hole mobility ($cm^2/V{\cdot}s$)	2.5	2.5	50	0.6
Electron lifetime (μs)	0.34	0.34	1	0.3
Hole lifetime (μs)	0.34	0.34	1	0.3
Acceptor concentration (cm^{-3})	0	0	0	0
Donor concentration (cm^{-3})	1×10^{18}	1×10^{18}	1×10^{15}	1×10^{15}
Effective conduction band density (cm^{-3})	2.2×10^{18}	2.2×10^{18}	4.42×10^{17}	1×10^{15}
Effective valence band density (cm^{-3})	1.8×10^{19}	1.8×10^{19}	8.72×10^{18}	1×10^{15}
Radiative recombination coefficient (cm^3/s)		/	3×10^{-13}	1×10^{-9}
Auger recombination coefficient (cm^6/s)		/	2×10^{-29}	1×10^{-20}
Surface recombination velocity (cm/s)		/	1	1, 10, 10^2, 10^3, 10^4, 10^5
Electron diffusion length (μm)		/	11.2	1.9
Hole diffusion length (μm)				1.7
Circuit series resistance (Ω/cm)			0	10
Circuit shunt resistance PSK (kΩ/cm)			Infinity	29.6
Circuit shunt resistance PET (kΩ/cm)			Infinity	22

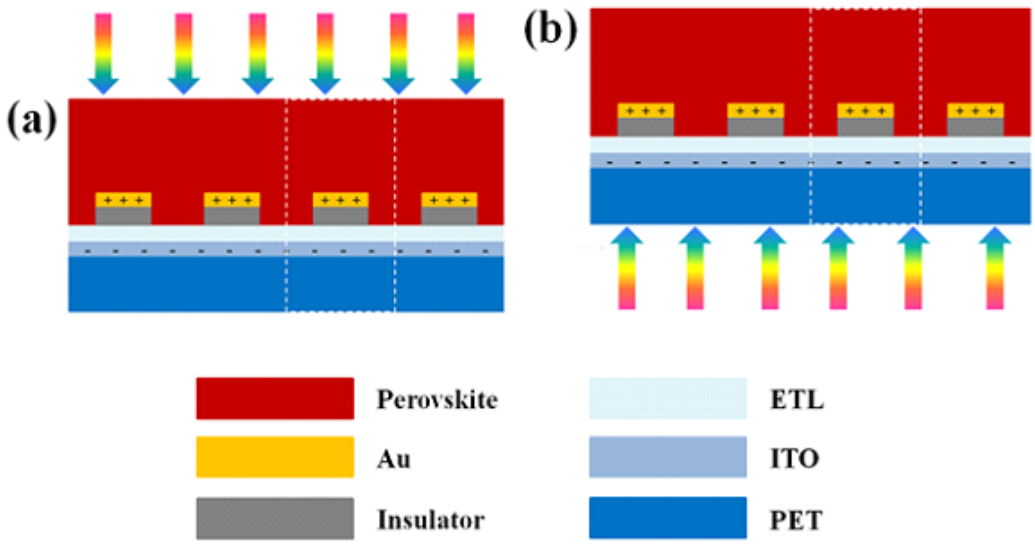

Figure S2. Sketch of the cross-section view (shown in xz-plane) of the sunlight fall on FQIBC PSCs from the fron- (perovskite-side) (a) and the rear-side (PET-side) (b). The areas enclosed with dashed white rectangles indicate the base unit areas used in simulation experiments.

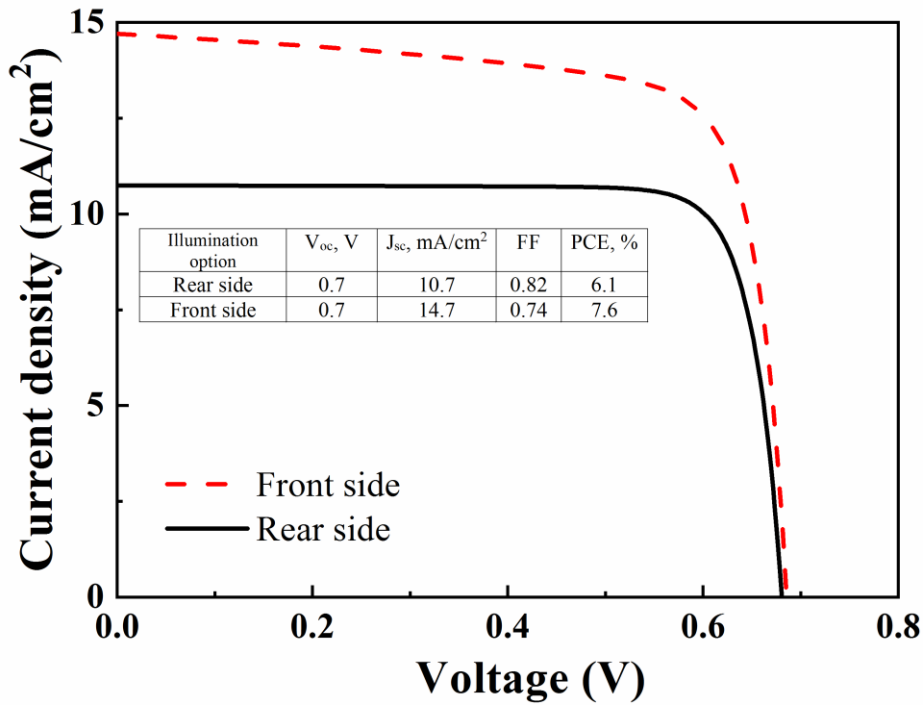

Figure S3. Comparison of the simulated *J-V* curves of FQIBC PSC for the front-side (dash red line) and the rear-side (solid black line) illumination.

Table S2. The calculated photovoltaic parameters of FQIBC PSCs under AM1.5G solar irradiation.

$S_{n,p}$, cm/s	Illumination option	V_{oc}, V	J_{sc}, mA/cm^2	*FF*	*PCE*, %
1	Front-side	0.69	9.7	0.39	2.6
1	Rear-side	0.69	9.5	0.4	2.1
10	Front-side	0.69	9.7	0.39	2.6
10	Rear-side	0.69	9.5	0.4	2.1
10^2	Front-side	0.69	8.3	0.39	2.26
10^2	Rear-side	0.69	6.6	0.46	2.1
10^3	Front-side	0.69	7.38	0.39	2.01
10^3	Rear-side	0.69	5.85	0.46	1.86
10^4	Front-side	0.65	3.48	0.37	0.85
10^4	Rear-side	0.68	4.21	0.42	1.2
10^5	Front-side	0.67	1.49	0.38	0.36
10^5	Rear-side	0.67	2.15	0.42	0.6

References:

1. Sze, S. M., Li, Y. & Ng, K. K. *Physics of Semiconductor Devices*. (John Wiley & Sons, 2021).
2. Hall, R. N. Electron-Hole Recombination in Germanium. *Phys. Rev.* **87**, 387–387 (1952).
3. Shockley, W. & Read, W. T. Statistics of the Recombinations of Holes and Electrons. *Phys. Rev.* **87**, 835–842 (1952).
4. Azri, F., Meftah, A., Sengouga, N. & Meftah, A. Electron and hole transport layers optimization by numerical simulation of a perovskite solar cell. *Sol. Energy* **181**, 372–378 (2019).
5. Hu, Y. *et al.* Perovskite solar cells with a hybrid electrode structure. *AIP Adv.* **9**, 125037 (2019).
6. Casas, G. A., Cappelletti, M. A., Cédola, A. P., Soucase, B. M. & Peltzer y Blancá, E. L. Analysis of the power conversion efficiency of perovskite solar cells with different materials as Hole-Transport Layer by numerical simulations. *Superlattices Microstruct.* **107**, 136–143 (2017).
7. Kiermasch, D., Rieder, P., Tvingstedt, K., Baumann, A. & Dyakonov, V. Improved charge carrier lifetime in planar perovskite solar cells by bromine doping. *Sci Rep* **6**, 39333 (2016).
8. Maynard, B. *et al.* Electron and hole drift mobility measurements on methylammonium lead iodide perovskite solar cells. *Appl. Phys. Lett.* **108**, 173505 (2016).

9. Kirchartz, T., Krückemeier, L. & Unger, E. L. Research Update: Recombination and open-circuit voltage in lead-halide perovskites. *APL Mater.* **6**, 100702 (2018).
10. Idígoras, J. *et al.* The Role of Surface Recombination on the Performance of Perovskite Solar Cells: Effect of Morphology and Crystalline Phase of TiO2 Contact. *Adv. Mater. Interfaces* **5**, 1801076 (2018).
11. Li, Y. *et al.* Direct Observation of Long Electron-Hole Diffusion Distance in CH3NH3PbI3 Perovskite Thin Film. *Sci Rep* **5**, 14485 (2015).